

VISCOSITY AND STRUCTURE EVOLUTION OF THE SiO₂-MgO-FeO-CaO-Al₂O₃ SLAG IN FERRONICKEL SMELTING PROCESS FROM LATERITE

X.-M. Lv, X.-W. Lv*, L.-W. Wang, J. Qiu, M. Liu

Chongqing University, School of Materials Science and Engineering, Chongqing, China

(Received 11 September 2015; accepted 30 December 2016)

Abstract

The SiO₂ fractions in laterite–nickel ores are quite high, thus certain amount of lime should be used as fluxing material to achieve good fluidity and desulfurization capacity in industrial smelting process. However, this operation leads to an additional cost of lime. In addition, the increase of slag volume decreases the effective furnace volume. To avoid such problem, partial reduction of FeO has been suggested. Therefore, the high SiO₂, low MgO and FeO and very little CaO slag is formed, which was less studied in the previous literature. Therefore, the viscosity and slag structure are investigated in the present study through FT–IR and Raman analysis methods. Experimental results show that the slag is a mixture of liquid and solid phases under the experimental temperature. The FT–IR and Raman spectra show that the fractions of the complex polymerization structure decrease significantly with the increase of FeO content and slag basicity, resulting in the decrease of apparent viscosity.

Keywords: Laterite–nickel ore; Slag structure; Viscosity; Basicity.

1. Introduction

Nickel sulfide and nickel laterite ores are two main resources for extracting nickel metal. With continuous decrease in high-grade sulfide nickel resource, the use of nickel laterite has drawn increasingly widespread attention [1–5]. Generally, the SiO₂ fraction in laterite is high, approximately 30 mass%–40 mass% [6]; hence, a certain amount of lime should be added into the slag to achieve good fluidity and desulfurization capacity in industrial smelting process. As a result, the cost of raw materials and the slag volume increases, the effective volume of the furnace decreases, thereby reducing the capability of the furnace. Less addition or no extra addition of lime can decrease the energy consumption and costs and improve the economic indicators of smelting to produce per ton nickel metal. However, less lime addition may increase the viscosity of the slag and result in poor separation of metal from the slag. To avoid such problem, partial reduction of the FeO has been suggested because more FeO remaining in the slag can improve viscosity. However, the viscosity of such slag has been less studied in previous literature. Therefore, this study investigated the viscosity and slag structure through FT–IR and Raman analysis. The results can approve the feasibility of the new slag style with low CaO.

2. Experimental

2.1. Experimental scheme

The slag samples were synthesized using reagent grade chemicals shown in Table 1. The basicity (MgO (mol%)/SiO₂ (mol%)) was set from 0.6 to 1.0. The FeO content in the slag was 5, 10, 15, 20, and 25 mass%.

Table 1. The chemical composition of the slag used/mass%

| Slag | MgO/SiO ₂ | MgO | SiO ₂ | Al ₂ O ₃ | CaO | FeO |
|------|----------------------|------|------------------|--------------------------------|-----|------|
| A1 | 0.6 | 24.4 | 61.1 | 5.0 | 1.5 | 8.0 |
| A2 | 0.7 | 27.2 | 58.3 | 5.0 | 1.5 | 8.0 |
| A3 | 0.8 | 29.7 | 55.8 | 5.0 | 1.5 | 8.0 |
| A4 | 0.9 | 32.1 | 53.4 | 5.0 | 1.5 | 8.0 |
| A5 | 1.0 | 34.2 | 51.3 | 5.0 | 1.5 | 8.0 |
| B1 | 0.9 | 33.2 | 55.3 | 5.0 | 1.5 | 5.0 |
| B2 | 0.9 | 31.3 | 52.2 | 5.0 | 1.5 | 10.0 |
| B3 | 0.9 | 29.4 | 49.1 | 5.0 | 1.5 | 15.0 |
| B4 | 0.9 | 27.6 | 45.9 | 5.0 | 1.5 | 20.0 |
| B5 | 0.9 | 25.7 | 42.8 | 5.0 | 1.5 | 25.0 |

*Corresponding author: lxuwei@163.com



2.2. Sample preparation

The slag used in this experiment was synthetic with pure chemical grade reagents ($\geq 99\%$ purity) provided by Shanghai Aladdin Co., Ltd. The slag composition was based on the chemical composition of nickel laterite ore used in the industry.

The reagents were weighed according to the required composition and mixed to become homogeneous. The mixtures were melted at $1550\text{ }^{\circ}\text{C}$ for 2 h in a MoSi_2 furnace under Ar atmosphere at a flow rate of 50 mL min^{-1} in a molybdenum (Mo) crucible (OD:52 mm, ID: 50 mm, Height: 100 mm). The Mo crucible was then placed in a corundum crucible; a graphite crucible was used as outer layer to remove the remaining oxygen in the furnace. Then the Mo crucible was rapidly removed from the furnace chamber and the slag sample was quickly poured into water. Afterwards, the quenched slag was dried in a muffle furnace and crushed to less than $100\text{ }\mu\text{m}$ for slag viscosity measurement. Two groups of quenched slag and slag after the viscosity testing were verified by chemical analysis which is shown in Table 2 and Table 3, which showed no significant composition change was observed, satisfying the requirement of the experiment.

Table 2. The chemical composition of quenched slag by XRF/mass%

| MgO/SiO ₂ | MgO | SiO ₂ | Al ₂ O ₃ | CaO | FeO |
|----------------------|-------|------------------|--------------------------------|------|------|
| 0.60 | 24.30 | 61.20 | 5.00 | 1.40 | 8.10 |
| 1.00 | 33.90 | 51.60 | 5.10 | 1.50 | 7.90 |

Table 3. The chemical composition of slag after the viscosity testing by XRF/mass%

| Series | MgO | SiO ₂ | Al ₂ O ₃ | CaO | FeO | MoO ₃ |
|--------|------|------------------|--------------------------------|-----|-----|------------------|
| A1 | 23.9 | 61.4 | 5.3 | 1.3 | 7.7 | 0.4 |
| A5 | 33.8 | 51.5 | 5.1 | 1.3 | 7.5 | 0.5 |

2.3. Experimental apparatus

In this study, the rotating cylinder method was employed for viscosity measurement. An electric resistance furnace with MoSi_2 heater used in this study was shown in Fig. 1. The torque was recorded using a rotating molybdenum spindle connected to a Brookfield digital viscometer (model LVDV-II+ Pro, USA). The furnace temperatures were controlled by the PID program. When the temperature reached the experimental temperature, the equilibration time for viscosity measurements was selected as 30 minutes. The average value of the viscosity data was calculated and recorded. The viscometer was calibrated at room temperature using standard oils of known viscosities (i.e., 0.96, 4.92 and 9.80 poise).

The structure of the investigated slag was analyzed by FT-IR spectroscopy (Nicolet, 5DXC, USA) and Raman spectroscopy (LabRAM HR Evolution; HORIBA Scientific, France). FT-IR transmitting spectra were recorded within $4000\text{--}400\text{ cm}^{-1}$ by using a spectrometer, equipped with a KBr detector. Each sample (2 mg) was mixed with 200 mg of KBr in an agate mortar, and then pressed into pellets with 13 mm diameter. The spectrum for each sample represents an average of 20 scans, which were normalized to the spectrum of the blank KBr pellet. The Raman spectra of the amorphous samples were obtained at room temperature within $100\text{--}1900\text{ cm}^{-1}$ with a 532 nm laser source [7-9].

2.4. Experimental procedure

The quenched slag was heated to $1550\text{ }^{\circ}\text{C}$ and held sufficiently for 120 minutes under 1.5 L min^{-1} of Argon flow in a Mo crucible to homogenize the slag, then the spindle was carefully immersed 5 mm deep into the molten slag and located in the middle of the slag because slight deviations of the spindle from the

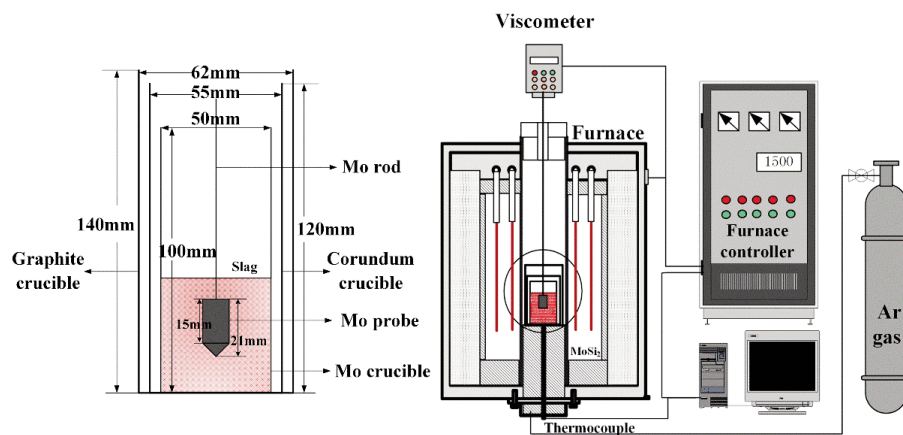


Figure 1. The schematic diagram of viscosity measurement system

central axis can easily produce errors. Viscosity were measured at every 20 °C from 1450 °C to 1550 °C with an equilibration time of 30 minutes and the torque values, which were stabilized for 2 min after the equilibrium time, were measured at a fix rotate speed of spindle (12 rpm), and the average value was used to determine the viscosity of molten slag. The standard deviations of viscosity were found to be less than ±0.02 poise.

3. Results and Discussion

3.1. Effect of basicity on viscosity

In the phase diagram calculated by FactSage 6.2 (Fig. 2), the red, green, and blue lines represent the liquid regions at 1550 °C, 1500 °C, 1450 °C, respectively. In which, each point describes the distribution of slag phase related to the slag composition shown in Table 1. Fig. 3 shows that the slag samples, except slag A2, exhibited a mixture of liquid and solid phases under 1450 °C, then the slag, except slag A5, melted into pure liquid phase with increasing temperature.

Fig. 3 shows the relationship between temperature and solid volume percent. The mass fraction of the suspended solutes or particles was calculated by FactSage 6.2 which is shown in Table 4, besides, the liquid slag and solid slag compositions can be obtained. Based on the calculated results, the solid slag consists mainly of Mg_2SiO_4 and a small amount of Fe_2SiO_4 , the densities of Mg_2SiO_4 and Fe_2SiO_4 are 3.22 g cm^{-3} , 4.40 g cm^{-3} , respectively, obtained by FactSage 6.2. The density of the liquid slag was obtained using the MLL Model [10] based on the liquid slag composition. The solid volume percent (ϕ) is calculated by the following equations:

$$V_s = M \times W_{s1} \div \rho_{s1} + M \times W_{s2} \div \rho_{s2} \quad \dots(1)$$

$$V_L = M \times W_L \div \rho_L \quad \dots(2)$$

$$\phi = \frac{V_s}{V_s + V_L} = \frac{W_{s1} \div \rho_{s1} + W_{s2} \div \rho_{s2}}{W_{s1} \div \rho_{s1} + W_{s2} \div \rho_{s2} + W_L \div \rho_L} \quad \dots(3)$$

where, M is the mass of the slag, V_s is the volume of solid slag, V_L is the volume of liquid slag, W_{s1} represents the mass fraction of Mg_2SiO_4 , W_{s2} represents the mass fraction of Fe_2SiO_4 , W_L represents the mass fraction of the liquid slag, ρ_{s1} is the density of Mg_2SiO_4 , ρ_{s2} is the density of Fe_2SiO_4 , ρ_L is the density of liquid slag.

The viscosity equation of the concentrated dispersion is described by Eq. (4), where η_r is the relative viscosity and ϕ is the volume fraction of the suspended solutes or particles assumed to be spherical [11]. Based on the concept, the viscosity of dispersion depends mainly on the size or the void volume of the suspended particles, irrespective of the particle shape. In addition, apparent spherical models for actual

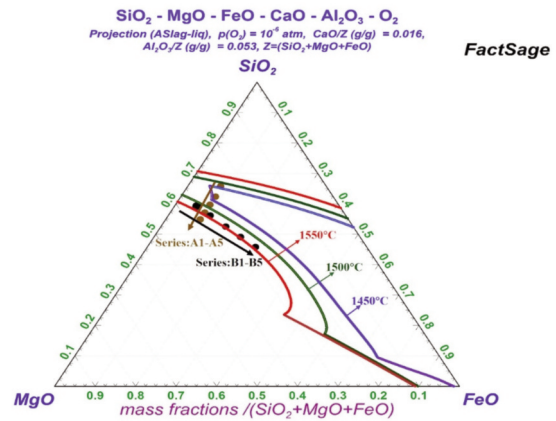


Figure 2. Phase diagram of SiO_2 - MgO - FeO - CaO - Al_2O_3

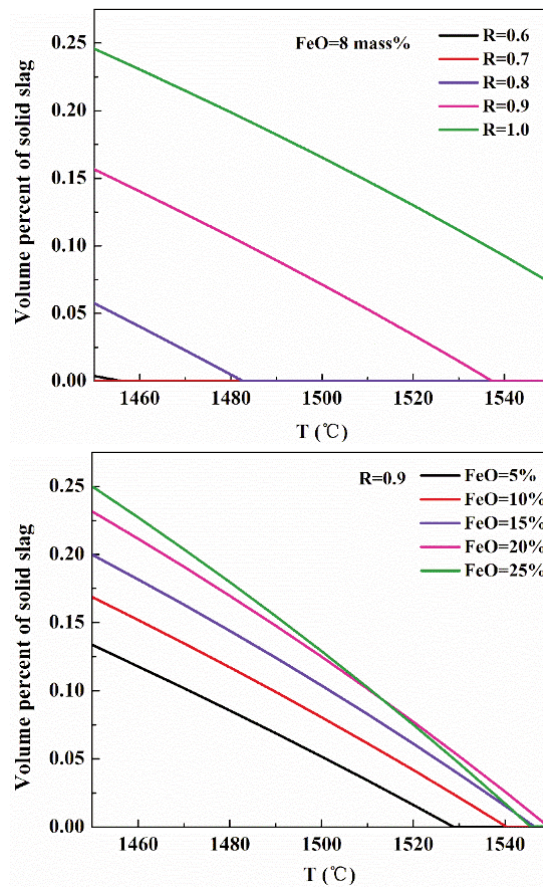


Figure 3. Relationship between temperature and solid volume percent

solutes or particles can be realized at any concentration in the treatment. The viscosity equation derived for dilute dispersion is extended to an equation applicable for dispersion at high concentrations. The flow pattern is assumed to be applicable for concentrated dispersions, including several particles, because the influence of the other



Table 4. The mass fraction of solid slag/mass%

| T/°C | A1 | A2 | A3 | A4 | A5 |
|------|-------|-------|-------|-------|-------|
| 1450 | 0.10 | 0.00 | 6.20 | 17.80 | 27.70 |
| 1470 | 0.00 | 0.00 | 2.00 | 14.00 | 24.30 |
| 1490 | 0.00 | 0.00 | 0.00 | 9.90 | 20.60 |
| 1510 | 0.00 | 0.00 | 0.00 | 5.70 | 16.70 |
| 1530 | 0.00 | 0.00 | 0.00 | 1.00 | 12.50 |
| 1550 | 0.00 | 0.00 | 0.00 | 0.00 | 8.00 |
| T/°C | B1 | B2 | B3 | B4 | B5 |
| 1450 | 15.70 | 18.70 | 20.80 | 22.50 | 22.20 |
| 1470 | 11.90 | 14.80 | 16.80 | 18.20 | 17.50 |
| 1490 | 8.00 | 10.70 | 12.40 | 13.50 | 12.40 |
| 1510 | 3.80 | 6.30 | 7.70 | 8.40 | 6.90 |
| 1530 | 0.00 | 1.60 | 2.70 | 2.90 | 1.00 |
| 1550 | 0.00 | 0.00 | 0.00 | 0.00 | 0.00 |

particles on the flow is small because of the canceling effects of the particles with one another. In this experiment, the volume fraction of the suspended solutes or particles was high, reaching up to 25 %. The effects of the particles on one another can be ignored because of the rotation of the viscometer rotor at high temperatures.

$$\eta_r = \frac{1-0.5\phi}{(1-\phi)^3} \quad (4)$$

The relationship of relative viscosity (η_r) between apparent viscosity (η) and viscosity of the slag that does not consider particles (η_L), is expressed as Eq. (5):

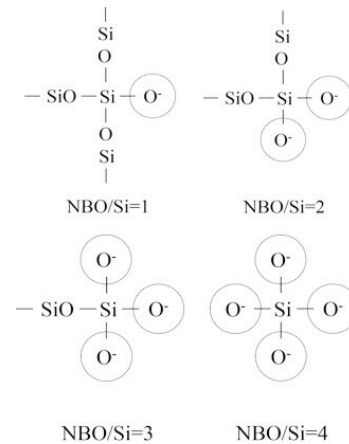
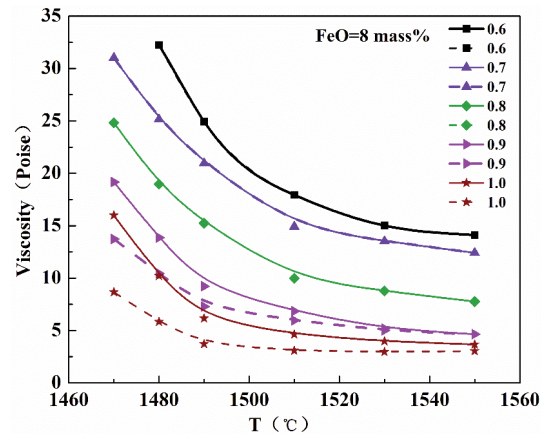
$$\eta_r = \frac{\eta}{\eta_L} \quad (5)$$

where η is the apparent viscosity and η_L is the viscosity of the slag, which does not consider the particles. According to the two equations, the viscosity of slag, which does not consider particles, can be obtained.

Fig. 5 shows the effect of basicity (MgO (mol%)/SiO₂ (mol%)) on viscosity in FeO of 8 mass%, from which two kinds of viscosities can be observed, the solid lines express the apparent viscosity, and the dashed lines represent the viscosity of the slag that does not consider the particles. Similarly, increased basicity decreased the viscosities of the two kinds of slag. In addition, the apparent viscosities of slags A4 and A5 is higher than the viscosity that does not consider particles because the presence of solid particles.

The structure of silicate melts is described in terms of anionic structural units that, on the average, have NBO/Si=1, 2, 3, and 4 (NBO/Si: non-bridging oxygen

per silicon) [12, 13]. The schematic illustration units with NBO/Si=1, 2, 3, and 4 is shown in Fig. 4. Basic oxides, such as MgO and CaO, influence the melt viscosity indirectly by influencing the silicon–oxygen anion structure. The apparent viscosity decreased from 33 poise to 16 poise as the basicity increases from 0.6 to 1.0 under 1450 °C, this observation indicates that higher MgO content has depolymerized the slag structure and decreased the slag viscosity by providing additional free oxygen ions (O²⁻) [14, 15].

**Figure 4.** Silicate structural units with NBO/Si=1, 2, 3, and 4**Figure 5.** Relationship between basicity and viscosity

3.2. Effect of FeO content on viscosity

Fig. 6 shows the viscosity of slag with FeO additions (5 mass%–20 mass%) and with a constant basicity of 0.9 at 1450 °C to 1550 °C, in which, the solid lines express the apparent viscosity and the dashed lines represent the viscosity of the slag that does not consider particles. In Fig. 6, the apparent viscosity of slag is higher than the viscosity that does not consider particles because of the presence of solid particles. Both the viscosities decreased with FeO addition because the basic oxide behavior of FeO

modified the network structure such as that of MgO [16]. The apparent viscosity decreased from 33 poise to 17 poise as the FeO content increases from 5 mass% to 25 mass% under 1450 °C, this indicates that higher FeO content is likely to depolymerize the slags silicate network structure into simpler polymer type units such as dimer or monomer [16] and decrease the viscosity.

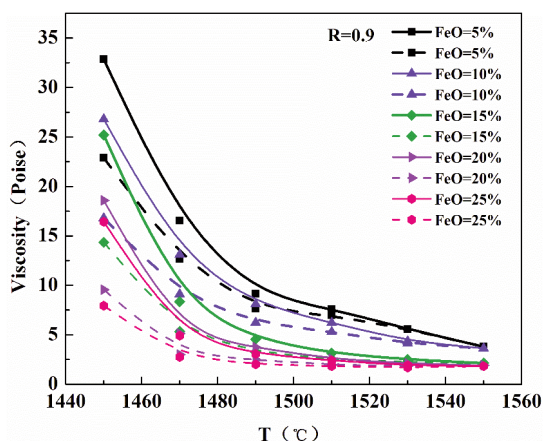


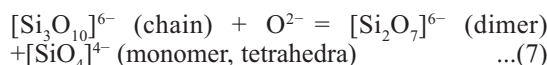
Figure 6. Relationship between FeO content and apparent viscosity

3.3. Analysis of IR spectra

Figs. 7 and 8 show the FT-IR results as a function of wavenumbers at different basicities and FeO contents and several kinds of band groups are observed from 1150 cm^{-1} to 400 cm^{-1} . The band group between 1100 and 850 cm^{-1} is related to the stretching vibration of silicate units containing $[\text{SiO}_4]$ -tetrahedra, the band group within 750–590 cm^{-1} is related to the stretching vibration of $[\text{AlO}_4]$ -tetrahedra and the Si–O bending trough was detected near 500 cm^{-1} [14, 18–20].

Several band groups of $[\text{SiO}_4]$ -tetrahedra with various NBO/Si were observed at about 1100–1050 (NBO/Si=1, sheets), 980–950 (NBO/Si=2, chains), 920–900 (NBO/Si=3, dimers), 880–850 cm^{-1} (NBO/Si=4, monomers) [14, 21] in Figs. 7 and 8. A broadening of the width of the Si–O band group is observed with increasing basicity and FeO content, which indicates the distance between Si and O increased, and the network structure was depolymerized [22]. In addition, with higher basicity and FeO content, the depths of the trough of NBO/Si=1 and 2 decreased and that of NBO/Si=3 and 4 increased, this indicates that higher MgO and FeO contents are likely to depolymerize the silicate network structure into simpler polymer type units such as dimer or monomer, which is further confirmed by Raman analysis.

Depolymerization of the slag structure of $[\text{Si}_3\text{O}_9]^{6-}$ (ring) (NBO/Si=2) units is shown as follows:



The band group within 750–590 cm^{-1} is related to the stretching vibration of $[\text{AlO}_4]$ -tetrahedra. However, no significant trough of $[\text{AlO}_4]$ -tetrahedra was found from the stretching vibration bands because of the low content (5 mass%) of Al_2O_3 in the slag series of A1 to B5. The Si–O bending trough was detected near 500 cm^{-1} , and the depth of the trough decreased with increasing basicity and FeO content as shown in Fig.7 and 8, and this indicates that the silicate structure has been depolymerized. Therefore, the FT-IR spectra suggests that MgO and FeO depolymerizes the slag by modifying the silicate structures.

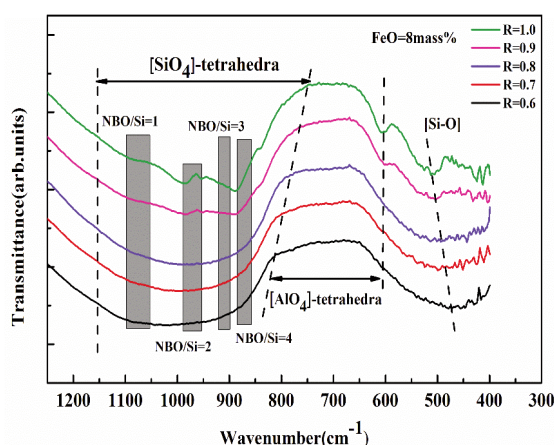


Figure 7. The effects of basicity on Infrared spectra of slag

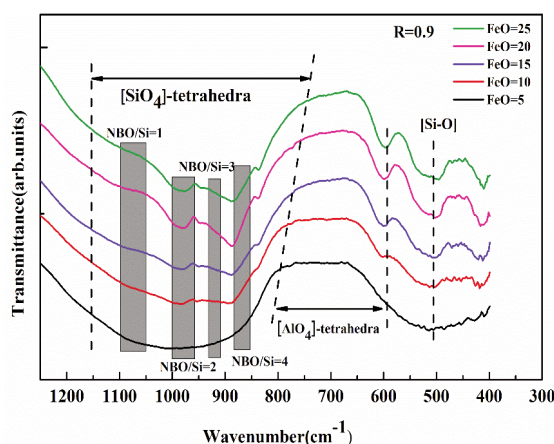


Figure 8. The effects of FeO content on Infrared spectra of slag

3.4. Analysis of Raman spectra

Raman analysis provides a quantitative measurement of the various silicate units as detailed in Table 5 unable to be verified by other spectroscopic methods. [22] In order to confirm the validity of



Raman spectra analysis, Si MAS-NMR technique was employed and the deconvoluted results are shown in Fig. 9 through the Gaussian-Deconvolution method by assuming contributions from structural units of NBO/Si=1, 2, 3, and 4 with the minimum correlation coefficient $r^2 \geq 0.998$ [23]. Because the slag A5 was a mixture of liquid and solid phases under 1550°C, the Raman spectra were used to analysis the slag structure of slag series of A1-A4. Fig. 9 shows the raw Raman spectra for the CaO-SiO₂-5 mass% Al₂O₃-CaO-8 mass% FeO slags with different basicities (0.6-0.9). In Fig. 9, several bands for [SiO₄]-tetrahedra peaks with various NBO/Si can be observed. It can be seen that two major peaks of NBO/Si of 2 and 4 increased, while that of NBO/Si of 1 and 3 decreased.

The relative fractions of the silicate units were plotted against basicity in Fig. 10. According to

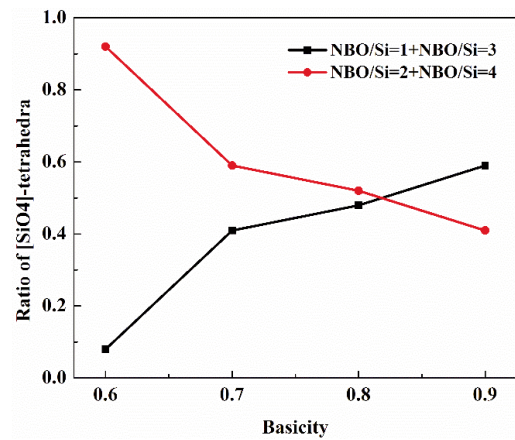


Figure 10. Ratio of [SiO₄]-tetrahedra with various NBO/Si as a function of basicity

Table 5. Raman active spectra vibrations for various silicate units

| Silicate unit | NBO/Si [Q notation] | Wavenumber (cm ⁻¹) | Vibrational Mode |
|--|---------------------|--------------------------------|-------------------|
| Si ₂ O ₅ ²⁻ | 1 (Q ³) | 1150-1050 | Symmetric stretch |
| Si ₂ O ₆ ⁴⁻ | 2 (Q ²) | 980-950 | Symmetric stretch |
| Si ₂ O ₇ ⁶⁻ | 3 (Q ¹) | 920-900 | Symmetric stretch |
| SiO ₄ ⁴⁻ | 4 (Q ⁰) | 880-850 | Symmetric stretch |

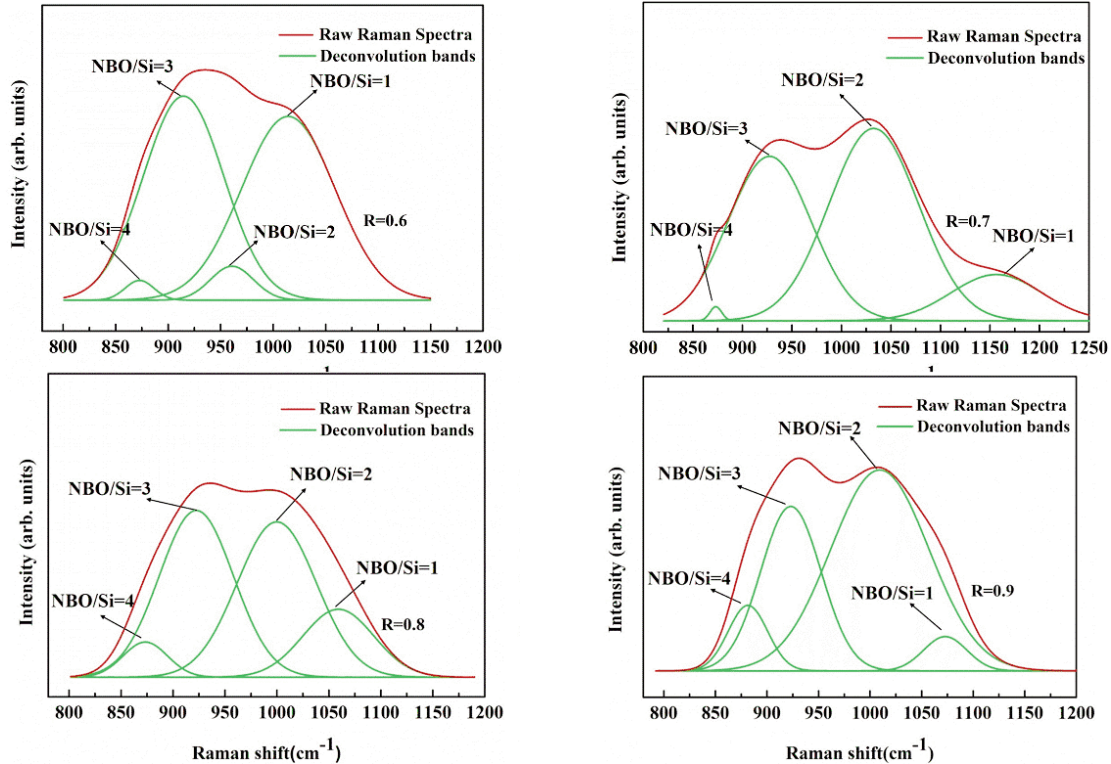


Figure 9. Deconvoluted results of the Raman spectral curves for slag A1-A4

Mysen et al. [21], the fractions of the structural units can be deduced from the areas of the corresponding Raman peaks, which are relevant to the structure of the melts. In Fig. 10, the fraction of NBO/Si of 1 and 3 decreased and that of NBO/Si of 2 and 4 increased with increasing basicity. This result suggests that MgO breaks the $[\text{SiO}_4]$ -tetrahedra network structure, declines the polymerization degree of silicon, and forms simpler melts. The depolymerization mechanism can be deduced to occur as reaction (8) [21]



Fig. 11 shows the raw Raman spectra for the CaO–SiO₂–5 mass% Al₂O₃–CaO based slags containing 5–25 mass% FeO. It can be seen that two major peaks of NBO/Si of 1 and 2 increased, while that of NBO/Si of

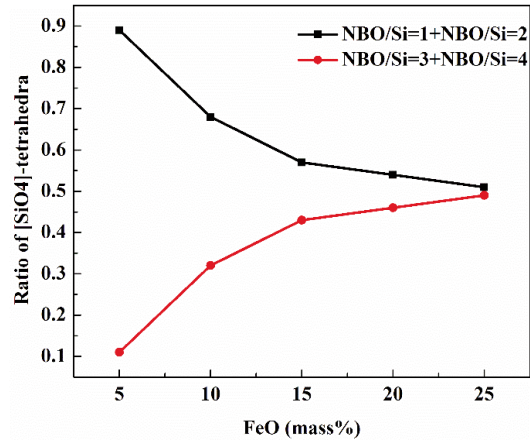


Figure 12. Ratio of $[\text{SiO}_4]$ -tetrahedra with various NBO/Si as a function of FeO content

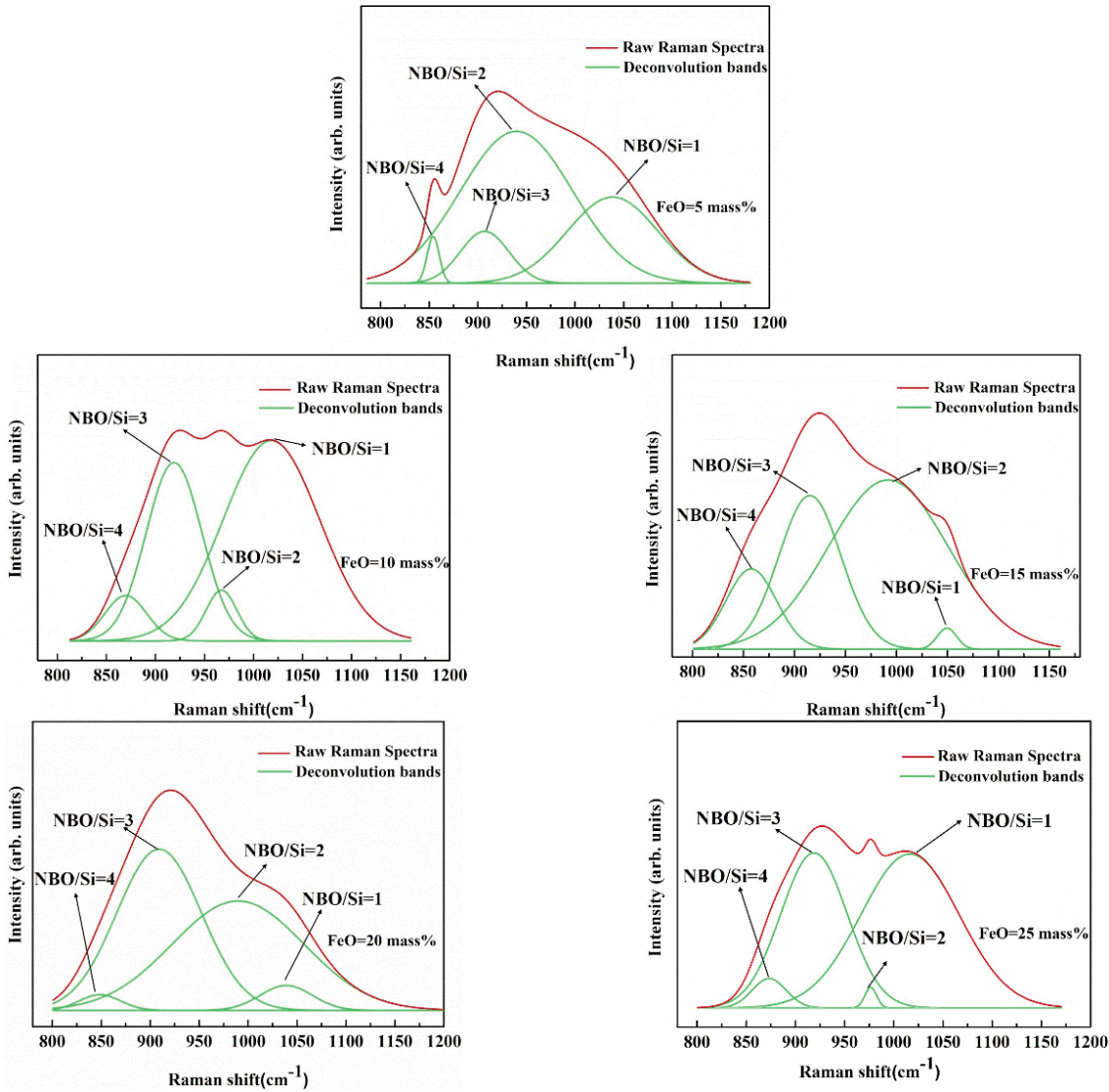


Figure 11. Deconvoluted results of the Raman spectral curves for slag B1-B5



3 and 4 decreased. Therefore, higher FeO content is likely to depolymerize $[\text{SiO}_4]$ -tetrahedra into simpler polymer type units such as dimers or monomers.

The effect of FeO content on the ratio of NBO/Si by Raman spectra can be observed in Fig. 12, in which, the fraction of NBO/Si of 1 and 2 decreased and that of NBO/Si of 3 and 4 increased with increasing FeO content. This result suggests that depolymerization occurred within the silicate structure and FeO broke the $[\text{SiO}_4]$ -tetrahedra network structure and formed simpler melts. Furthermore, the fraction of NBO/Si of 1 and 2 significantly decreased as the FeO content increases from 5 mass% to 15 mass%, but decreased slightly with FeO content increasing from 15 mass% to 25 mass%. This results correspond well with the viscosity changes shown in Fig. 6.

4. Conclusions

(1) Slag viscosity was measured by the rotating cylindrical method from 1450 °C to 1550 °C. The results showed that the slag was a mixture of liquid and solid phases under the experimental temperature.

(2) Viscosity decreases with increasing basicity and FeO content, but decreases obviously when the FeO content increases from 5 mass% to 15 mass%.

(3) Higher basicity or FeO content is likely to depolymerize $[\text{SiO}_4]$ -tetrahedra into simpler polymer type units such as dimers or monomers, and decreased the viscosity.

Acknowledgments

The authors are especially grateful to The National Natural Science Foundation of China (No.51234010).

References

- [1] X. M. Li, L. Tang, S. L. Liu, *Ferro-Alloys*, (4) (2007) 24-28.
- [2] X. Y. Guo, Z. Wu, D. Li, *Metal Materials and Metallurgy Engineering*, 37 (2) (2009) 3-9.
- [3] J. B. Chen, J. H. Xu, *Express Information of Mining Industry*, (8) (2006) 1-3+37.
- [4] Y. Jiang, M. X. Hou, *Nonferrous Mining and Metallurgy*, 24 (2) (2008) 55-57.
- [5] S. W. Zhang, S. B. Xie, A. D. Xu, *World Nonferrous Metals*, (11) (2003) 9-14.
- [6] Y. P. Zhang, Y. S. Zhou, Z. Y. Li, W. G. Li, *Ferro-Alloys*, (6) (2007) 18-21.
- [7] P. Mcmilla, *American Mineralogist*, 69 (7-8) (1984) 622-644.
- [8] K. Zheng, J. Liao, X. Wang, *Journal of Non-Crystalline Solids*, 376 (10) (2013) 209-215.
- [9] J. H. Park, *Metall Mater Trans B*, 44 (4) (2013) 938-947
- [10] K. Mills, *The estimation of slag properties*, Southern African Pyrometallurgy, London, 2011, p. 20-21.
- [11] K. Toda, H. Furuse, *Bioscience and Bioengineer*, 102 (6) (2006) 524-528.
- [12] S. Ueda, H. Koyo, T. Ikeda, Y. Kariya, M. Maeda, *ISIJ Int.*, 40 (2000), 739-743.
- [13] S. Kashio, Y. Iguchi, T. Goto, Y. Nishina, *Trans. Iron Steel Inst. Jpn.*, 20 (1980), 251-253.
- [14] H. Park, J. Y. Park, G. H. Kim, I. Sohn, *Steel Res. Int.*, 83 (2012) 150-156.
- [15] B. O. Mysen, *Earth-Science Reviews*, 27 (4) (1990) 281-365.
- [16] J. R. Kim, Y. S. Lee, D. J. Min, *Isij Int.*, 44 (8) (2004) 1291-1297.
- [17] K. Mills, *Isij Int.*, 46 (1) (2006) 50-57.
- [18] H. Kim, W. H. Kim, I. Sohn, D. J. Min, *Steel Res. Int.*, 81 (2010) 261-264.
- [19] S. M. Han, J. G. Park, I. Sohn, *J. Non-Cryst. Solids*, 357 (2010) 2868-2872.
- [20] S. Agathopoulos, D. U. Tulyaganov, J. M. G. Ventura, *J. Non-Cryst. Solids*, 352 (2006) 322-326.
- [21] B. O. Mysen, D. Virgo, C.M. Scarfe, *Am. Mineral.*, 65 (1980) 690-710.
- [22] F. Rouessac, A. Rouessac, *Chemical Analysis - Modern Instrumentation Methods and Techniques*, John Wiley and Sons Inc., West Sussex, 2007, p. 207-214.
- [23] J.L. Li, Q.F. Shu, K.C. Chou, *ISIJ Int.*, 54 (2014) 721-727.

